

# Hoxa5 increases mitochondrial apoptosis by inhibiting Akt/mTORC1/S6K1 pathway in mice white adipocytes

Fei Feng<sup>1</sup>, Qian Ren<sup>1</sup>, Song Wu<sup>1</sup>, Muhammad Saeed<sup>1</sup> and Chao Sun<sup>1</sup>

<sup>1</sup>College of Animal Science and Technology, Northwest A&F University, Yangling, Shaanxi 712100, China

Correspondence to: Chao Sun, email: sunchao2775@163.com

Keywords: *Hoxa5*; white adipocytes; mitochondrial apoptosis; mice; Akt/mTORC1 pathway

Received: June 20, 2017

Accepted: August 04, 2017

Published: August 24, 2017

Copyright: Feng et al. This is an open-access article distributed under the terms of the Creative Commons Attribution License 3.0 (CC BY 3.0), which permits unrestricted use, distribution, and reproduction in any medium, provided the original author and source are credited.

## ABSTRACT

**Homeobox A5 (*Hoxa5*), a member of the *Hox* family, plays a important role in the regulation of proliferation and apoptosis in cancer cells. The dysregulation of the adipocyte apoptosis *in vivo* leads to obesity and metabolic disorders. However, the effects of *Hoxa5* on adipocyte apoptosis are still unknown. In this study, palmitic acid (PA) significantly increased the mRNA level of *Hoxa5* and triggered white adipocyte apoptosis *in vivo* and *in vitro*. Further analysis revealed that *Hoxa5* enhanced the early and late apoptotic cells and fragmentation of genomic DNA in adipocytes from inguinal white adipose tissue (iWAT) of mice. Moreover, *Hoxa5* aggravated white adipocyte apoptosis through mitochondrial pathway rather than endoplasmic reticulum stress (ERS)-induced or death receptor (DR)-mediated pathway. Our data also confirmed that *Hoxa5* promoted mitochondrial apoptosis pathway by elevating the transcription activity of *Bax* and inhibiting the protein kinase B (Akt)/mammalian target of rapamycin complex 1 (mTORC1) signaling pathway. In summary, these findings revealed a novel mechanism that linked *Hoxa5* to white adipocyte apoptosis, which provided some potential possibilities to prevent and treat obesity and some metabolic diseases.**

## INTRODUCTION

*Hoxa5* protein is a member of the *Hox* protein family and is an important transcription factor which plays a definitive role in patterning the cells and tissues, especially the anteroposterior body axis during embryogenesis [1–3]. And *Hoxa5* is known to be associated with the process of cell proliferation, migration and apoptosis in cancer cells [4–6]. Previous studies have shown that abnormal expression of some *Hox* genes in multiple cancer types [7]. Raman et al. (2000) have found that *Hoxa5* expression is low in breast cancer cell lines and forced-expression of *Hoxa5* induces apoptosis [8, 9]. Moreover, *Hoxa5* could increase apoptosis by p53-dependent or p53-independent pathway, especially in cancer cells, such as breast cancer cells, epithelial cancer cells, lipoma cells and lung cancer cells [10, 11]. In addition, retinoid acid (RA) bound to retinoid acid receptors (RARs) and transcriptionally

activated *Hoxa5*, which was important for RA-mediated apoptosis increase and proliferation inhibition in a variety of breast cancer cells [12, 13].

Akt/mTOR signaling pathway is essential for multiple cellular processes, such as cell proliferation, apoptosis, cell migration, differentiation and glucose metabolism [14–17]. Current evidences suggest that Akt signaling pathway plays a critical role in regulating *Hox* gene expression during RA-induced apoptosis [18, 19]. Knockdown of some *Hox* genes inhibited activation of extracellular regulated protein kinases 1/2 (ERK1/2) and Akt pathway in prostate cancer cells [20]. These findings implied that *Hoxa5* might act as an important mediator of several pathways in coordinating apoptosis.

Obesity is a complex chronic disease and it increases risk for human health by causing type 2 diabetes, fatty liver, hyperlipidemia and other metabolic disorders. Moreover, obesity is determined by the number and volume of

adipocytes in adipose tissue, which depends on the balance between cell survival and apoptosis [21–23]. Previous studies have found that PA induced dysfunction and apoptosis by activating reactive oxygen species (ROS) generation in pancreatic  $\beta$ -cells and podocytes. And PA could trigger mouse preadipocyte apoptosis by increasing cysteinyl aspartate specific proteinase (caspase) cascade reaction [24–26]. Some researchers have found that in epididymal adipose tissue of mice fed with a high-fat diet (HFD), *Hoxa5* undergoes dynamic DNA methylation and transcriptional repression, which may represent a potential way to quantify obesity response to nutritional intervention [27]. However, recent studies about *Hoxa5* mainly focus on cancer cells and the precise molecular mechanisms involved in the regulation of *Hoxa5* on adipocyte apoptosis are unclear.

In this study, we investigated the effects of *Hoxa5* on white adipocyte apoptosis. We have shown that *Hoxa5* increased apoptosis by inhibiting Akt/mTORC1 signaling pathway in white adipocytes of mice. In addition, *Bax*, as a target of *Hoxa5*, was very important in *Hoxa5*-induced apoptosis through mitochondrial pathway. And these findings might open new therapeutic possibilities against obesity and type 2 diabetes.

## RESULTS

### PA triggered apoptosis along with the increased *Hoxa5* mRNA level in white adipose tissue of mice

Our result showed that body weight was decreased after intraperitoneal injection of PA ( $P < 0.05$ ), while there was no difference in food intake (Figure 1A and 1B). PA treatment increased the mRNA level of *Hoxa5* in both inguinal white adipose tissue (iWAT) and interscapular brown adipose tissue (iBAT) ( $P < 0.05$ ), but did not change the expression of *Hoxa4*, *Hoxa7* and *Hoxa9* in iWAT compared with those in iBAT (Figure 1C). We then measured the mRNA levels of *Bax*, *Bcl-2*, *Caspase-9* and *Caspase-3*, and data showed PA significantly increased the mRNA levels of pro-apoptotic genes ( $P < 0.05$ ) (Figure 1D). Additionally, mice white adipocytes from iWAT were incubated with 250 nM PA for 24 h. Our results demonstrated PA reduced adipocyte viability ( $P < 0.05$ ) and increased the number of apoptotic cells (Figure 1E and 1F). Interestingly, PA also elevated the mRNA level of *Hoxa5* ( $P < 0.05$ ) and triggered white adipocyte apoptosis by promoting the expression of *Bax*, *Caspase-9* and *Caspase-3*, but suppressing *Bcl-2* ( $P < 0.05$ ) (Figure 1G). Similarly, serum-free medium treatment also induced white adipocyte apoptosis and increased the mRNA level of *Hoxa5* ( $P < 0.05$ ) (Figure 1H–1J). Thus, PA triggered apoptosis in white adipose tissue along with a higher level of *Hoxa5*. So, we speculated *Hoxa5* might increase white adipocytes apoptosis in mice.

### *Hoxa5* increased apoptosis of white adipocytes

Mice white adipocytes were infected with adenovirus overexpression vector of *Hoxa5* (Ad-*Hoxa5*) or adenovirus interference vector of *Hoxa5* (sh-*Hoxa5*). We found there were no difference between Ad-GFP and negative control in *Hoxa5* mRNA and protein level ( $P > 0.05$ ). Compared with the control group, Ad-*Hoxa5* and sh-*Hoxa5* were functional (Figure 2A). As shown in Figure 2B, Ad-*Hoxa5* elevated the number of apoptotic adipocytes with Hoechst staining. In addition, Annexin V/PI staining and an analysis by flow cytometry showed a higher percentage of apoptotic cells in the early and late stage after Ad-*Hoxa5* treatment as compared with control group ( $P < 0.05$ ) (Figure 2C). Further, we detected the fragments of genome DNA in nucleus with TUNEL staining, indicating that overexpression of *Hoxa5* increased the number of TUNEL-positive cells ( $P < 0.05$ ), while the knockdown group had less positive cells ( $P < 0.05$ ) (Figure 2D). Western blot analysis showed that *Hoxa5* also enhanced the protein level of active Caspase-3 ( $P < 0.05$ ) (Figure 2E). Together, these data suggested that *Hoxa5* suppressed survival and promoted the apoptosis process of white adipocytes.

### *Hoxa5* promoted apoptosis through mitochondrial pathway in white adipocytes

Next, we addressed how *Hoxa5* increased apoptosis in mice white adipocytes. Hoechst staining analysis showed Ad-*Hoxa5* treatment markedly enhanced apoptotic cells (Figure 3A). And as expected, cell viability was decreased in Ad-*Hoxa5* group ( $P < 0.05$ ) (Figure 3B). However, further analysis demonstrated there were no change in mRNA levels of *FasL*, *TNF- $\alpha$* , *caspase-2* and *caspase-8* of white adipocytes ( $P > 0.05$ ), which were key genes regulating the DR-mediated apoptosis pathway (Figure 3C). And our data showed ERS marker genes *Grp78* and *Chop* were both elevated after tunicamycin (TM) treatment ( $P < 0.05$ ) and further measurements indicated that TM treatment triggered apoptosis of white adipocytes by increasing the mRNA levels of *Caspase-12* ( $P < 0.05$ ) and *Caspase-7* ( $P < 0.01$ ). Interestingly, *Hoxa5* did not change these marker genes of the ERS-induced apoptotic pathway ( $P > 0.05$ ) (Figure 3D). Then, to examine how *Hoxa5* increased apoptosis in mice white adipocytes, we tested mitochondrial membrane potential. JC-1 staining and flow cytometry analysis showed that Ad-*Hoxa5* treatment lowered the ratio of red/green fluorescence intensity compared with control group ( $P < 0.01$ ) (Figure 3E). Moreover, Ad-*Hoxa5* treatment significantly increased ( $P < 0.05$ ) Cytochrome-c (Cyt-c) protein (Figure 3F), which bound to apoptotic protease activating factor-1 (Apaf-1), forming an apoptosome complex with procaspase-9 and subsequently activated downstream effector caspases to induce apoptosis. Those changes were correlated with the increase of mitochondrial

pro-apoptotic markers *Bax* ( $P < 0.05$ ), *Bid* ( $P < 0.05$ ), *Bad* ( $P < 0.01$ ), *Caspase-9* ( $P < 0.05$ ), *Caspase-3* ( $P < 0.05$ ) and the reduction of mitochondrial anti-apoptotic marker *Bcl-2* ( $P < 0.05$ ) after forcing expression of *Hoxa5* (Figure 3G). Our above data collectively revealed *Hoxa5* increased adipocyte apoptosis through mitochondrial pathway, but not other pathways, such as ERS-induced and DR-mediated pathway.

### **Hoxa5 aggravated PA- and serum starvation-induced white adipocyte apoptosis**

We then studied the function of *Hoxa5* in two different models of apoptosis to further verify the pro-apoptotic effects of *Hoxa5*. White adipocytes were incubated with 250 nM PA for 24 h or serum-free medium for 12 h. Our data demonstrated that PA increased the mRNA levels of *Bax*, *Caspase-3* and *Caspase-9*, but reduced *Bcl-2* ( $P < 0.05$  or  $P < 0.01$ ). The combination with

forced expression of *Hoxa5* also increased the mRNA and protein level of pro-apoptotic genes ( $P < 0.05$ ) (Figure 4A and 4B). Similarly, overexpression of *Hoxa5* aggravated starvation-induced adipocyte apoptosis as well. A higher mRNA ( $P < 0.05$ ) and protein level of *Bax* ( $P < 0.01$ ), increased protein level of active caspase-3 ( $P < 0.01$ ) and reduced mRNA and protein level of *Bcl-2* ( $P < 0.05$ ) indicated that adipocyte apoptosis was successfully aggravated by a high expression of *Hoxa5* (Figure 4C and 4D). The above data demonstrated *Hoxa5* promoted the process of PA- and serum starvation-induced apoptosis in white adipocytes, further verifying the pro-apoptotic effect of *Hoxa5*.

### **Hoxa5 promoted apoptosis by elevating *Bax* transcription in white adipocytes**

Analysis of our online prediction demonstrated that the *Bax* promoter contained an important binding site,

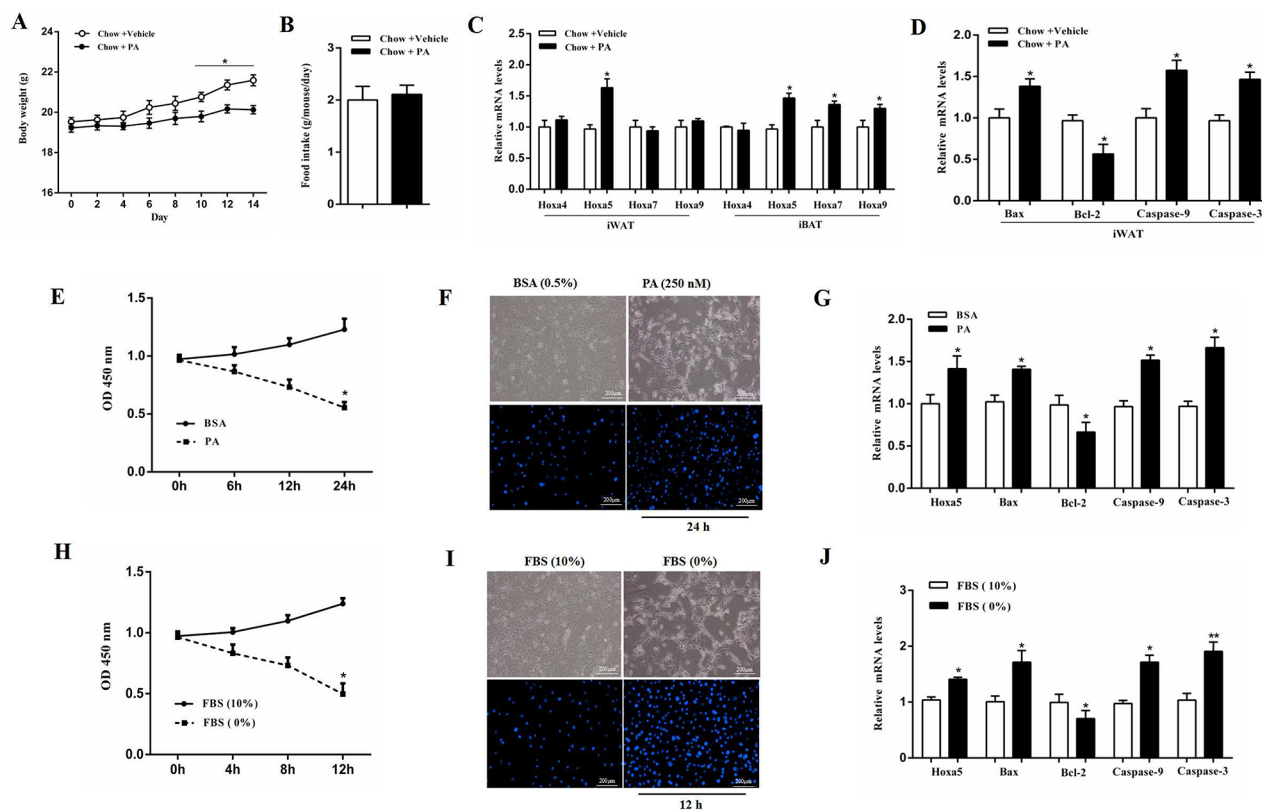


**Figure 1: PA triggered apoptosis along with the increased *Hoxa5* mRNA level in white adipose tissue of mice.** (A) Body weight of mice fed on chow diet after palmitate acid (PA, 1  $\mu\text{g/g}$ ) injection per 2 days during 2 weeks ( $n = 6$ ). (B) Food intake of mice fed on chow diet after PA injection ( $n = 6$ ). (C, D) Relative mRNA levels of *Hoxa4*, *Hoxa5*, *Hoxa7* and *Hoxa9* in iBAT and *Hoxa4* and *Hoxa9* in iBAT (C) and relative mRNA levels of *Bax*, *Bcl-2*, *Caspase-9* and *Caspase-3* in iBAT (D) of mice fed on chow diet after PA injection on the 14<sup>th</sup> day ( $n = 6$ ). (E) Relative OD values for cell viability of white adipocytes after 250 nM PA incubation for 6, 12 and 24 h ( $n = 6$ ). (F) Hoechst 33258 staining of white adipocyte apoptosis after PA incubation for 24 h. Scale bar: 200  $\mu\text{m}$  ( $n = 3$ ). (G) Relative mRNA levels of *Hoxa5*, *Bax*, *Bcl-2*, *Caspase-9* and *Caspase-3* in white adipocytes after PA incubation for 24 h ( $n = 6$ ). (H) Relative OD values for cell viability of white adipocytes after serum starvation for 4, 8 and 12 h ( $n = 6$ ). (I) Hoechst 33258 staining of white adipocyte apoptosis after serum starvation for 12 h. Scale bar: 200  $\mu\text{m}$  ( $n = 3$ ). (J) Relative mRNA levels of *Hoxa5*, *Bax*, *Bcl-2*, *Caspase-9* and *Caspase-3* in white adipocytes after serum starvation for 12 h ( $n = 6$ ). Values are mean  $\pm$  SEM. \* $P < 0.05$ , \*\* $P < 0.01$  compared with the control.

129 bp - 111 bp upstream of the initiation codon of *Bax*, which was the potential target of *Hoxa5* (Figure 5A). Mutation of the binding site in the *Bax* promoter reduced the *Bax* transcription activity ( $P < 0.01$ ) (Figure 5B). We then treated cells with the overexpression of *Hoxa5*, and the result showed that *Hoxa5* overtly enhanced the level of *Bax* transcription ( $P < 0.01$ ) (Figure 5B). Additionally, the transcriptional regulation between *Hoxa5* and *Bax* was also verified by the ChIP measurement ( $P < 0.05$ ) (Figure 5C). And Figure 5D showed that Ad-*Hoxa5* significantly increased the mRNA levels of *Hoxa5* ( $P < 0.01$ ) and *Bax* ( $P < 0.05$ ) in white adipocytes. Then, further investigation found that overexpression of *Hoxa5* elevated the mRNA levels of *Bax* and *Caspase-3* ( $P < 0.05$ ), but reduced *Bcl-2* ( $P < 0.05$ ) in *Bax* interference group (Figure 5E and 5F). Together, the data strongly suggested *Hoxa5* controlled apoptosis by elevating *Bax* transcription level in white adipocytes.

## *Hoxa5* increased white adipocyte apoptosis via the Akt/mTORC1 pathway

To further dissect the possible molecular mechanism of *Hoxa5* on the adipocyte apoptosis, we determined whether *Hoxa5* regulate the mTOR pathway in white adipocytes. We found reduced phosphorylation levels of Akt at Ser473, mTORC1 at Ser2448 and ribosome protein subunit 6 kinase 1 (S6K1) at Thr389 in the *Hoxa5* forced expression group compared to the control ( $P < 0.05$ ) (Figure 6A and 6C), suggesting that *Hoxa5* disturbed the mTORC1 signaling pathway, involving the upstream and downstream targets. Along with the inactivation of mTORC1 signaling pathways, *Hoxa5* increased the protein levels of active caspase-3 and reduced Bcl-2 ( $P < 0.05$ ) (Figure 6B and 6D). Thus, these results suggest that *Hoxa5* triggered the adipocyte apoptosis by inhibiting mTORC1 signaling pathway. We then further

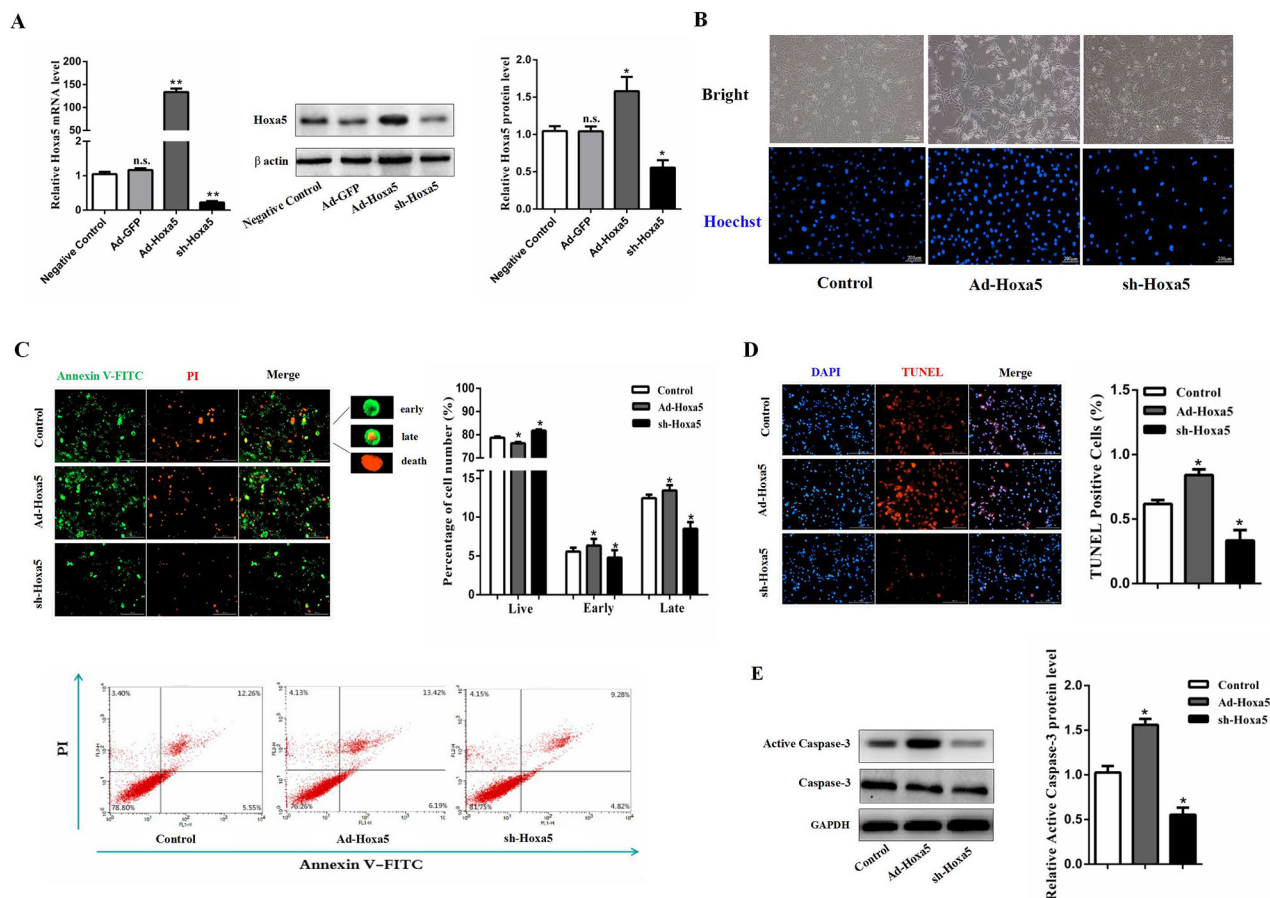


**Figure 2: *Hoxa5* increased apoptosis of white adipocytes.** White adipocytes were pretreated with either Ad-*Hoxa5* or sh-*Hoxa5*. (A) Efficiencies of Ad-*Hoxa5* or sh-*Hoxa5* in white adipocytes ( $n = 6$ ). (B) Hoechst 33258 staining of white adipocyte apoptosis. Scale bar: 200  $\mu\text{m}$  ( $n = 3$ ). (C) Annexin V-FITC/PI double staining and flow cytometry analysis of white adipocyte apoptosis. Scale bar: 200  $\mu\text{m}$  ( $n = 3$ ). (D) TUNEL staining of DNA fragments in white adipocytes. Scale bar: 200  $\mu\text{m}$  ( $n = 3$ ). (E) Relative protein level of active Caspase-3 in white adipocytes ( $n = 3$ ). Values are mean  $\pm$  SEM. \* $P < 0.05$ , \*\* $P < 0.01$  compared with the control.

studied whether these effects were affected by Akt/mTORC1 signaling. Treatment with the Akt inhibitor MK2206 significantly reduced the phosphorylation level of Akt at Ser473 ( $P < 0.05$ ) (Figure 6A). MK2206 also decreased the phosphorylation level of the downstream target, mTORC1, at Ser2448 ( $P < 0.05$ ) and the protein level of Bcl-2 ( $P < 0.05$ ), but elevated activity of cleaved caspase-3 ( $P < 0.05$ ) (Figure 6A and 6B). So, Hoxa5 aggravated the effect of MK2206 on apoptosis. Moreover, we observed a lower phosphorylation levels of mTORC1 at Ser2448 ( $P < 0.01$ ) and S6K1 at Thr389 ( $P < 0.05$ ) when we treated adipocytes with rapamycin, a specific phosphorylation inhibitor of mTORC1 (Figure 6C). And

rapamycin increased the activity of cleaved caspase-3 ( $P < 0.05$ ) and reduced the protein level of Bcl-2 ( $P < 0.05$ ) (Figure 6D). Similarly, Hoxa5 aggravated the effect of rapamycin on apoptosis. Collectively, these data provided evidence to suggest that Hoxa5 increased apoptosis of white adipocytes by inhibiting the Akt/mTORC1/S6K1 signaling pathway.

### Hoxa5 promoted PA-induced apoptosis in white adipose tissue of mice

We next intraperitoneally injected Ad-Hoxa5 or sh-Hoxa5 to investigate the role of Hoxa5 in PA-induced

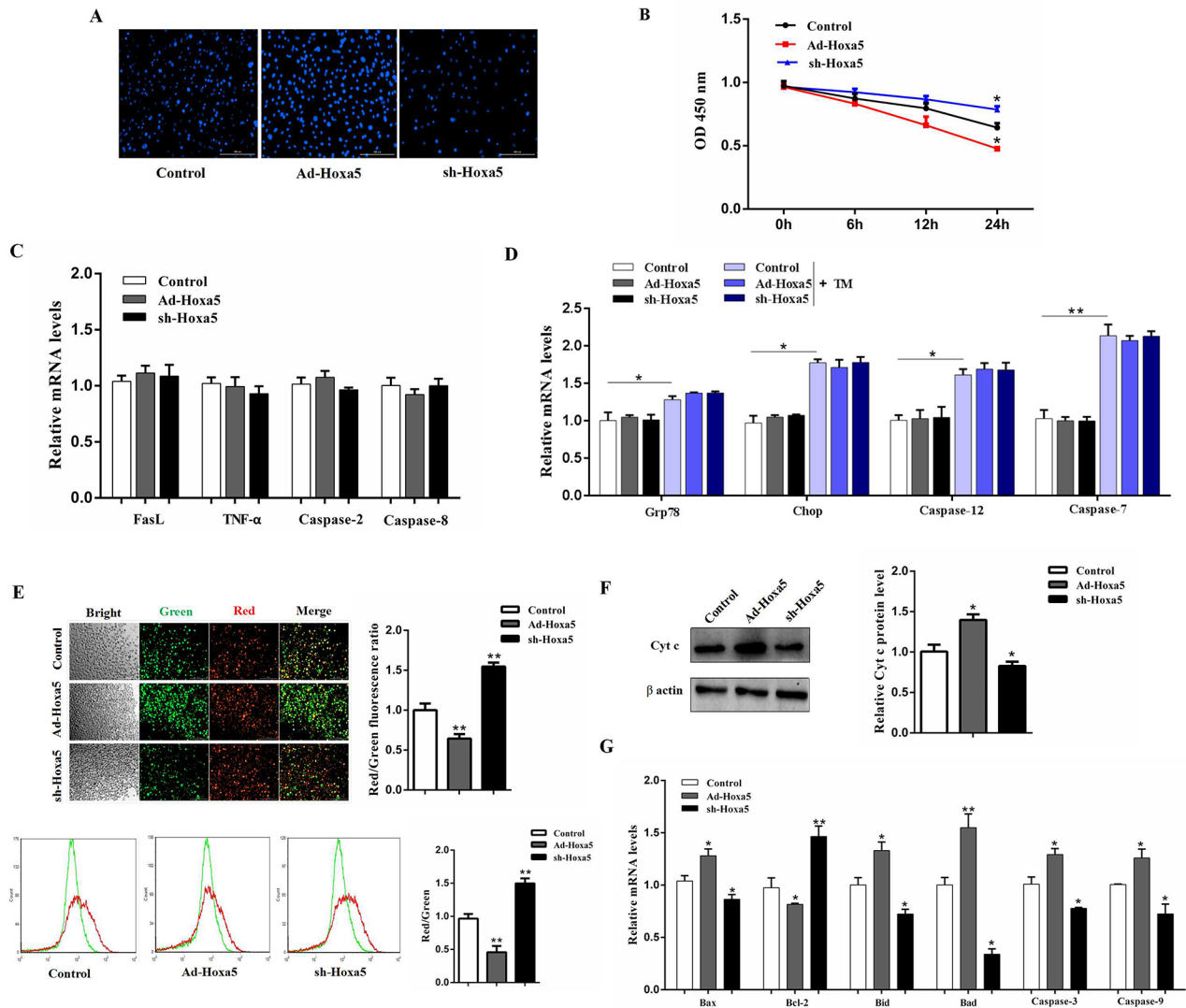


**Figure 3: Hoxa5 promoted apoptosis through mitochondrial pathway in white adipocytes.** White adipocytes were pretreated with either Ad-Hoxa5 or sh-Hoxa5. (A) Hoechst 33258 staining of white adipocyte apoptosis for 24 h. Scale bar: 200  $\mu$ m ( $n = 3$ ). (B) Relative OD values for cell viability of white adipocytes for 6, 12 and 24 h ( $n = 6$ ). (C, D) Relative mRNA levels of *FasL*, *TNF- $\alpha$* , *Caspase-2*, *Caspase-8* (C), *Grp78*, *Chop*, *Caspase-12* and *Caspase-7* (D) ( $n = 6$ ). (E) JC-1 staining and flow cytometry analysis for mitochondrial membrane potential of white adipocytes. Scale bar: 200  $\mu$ m ( $n = 3$ ). (F) Relative protein level of Cytochrome-c (Cyt-c) in white adipocytes ( $n = 3$ ). (G) Relative mRNA levels of *Bax*, *Bcl-2*, *Bid*, *Bad*, *caspase-3* and *caspase-9* in white adipocytes ( $n = 6$ ). Values are mean  $\pm$  SEM. \* $P < 0.05$ , \*\* $P < 0.01$  compared with the control.

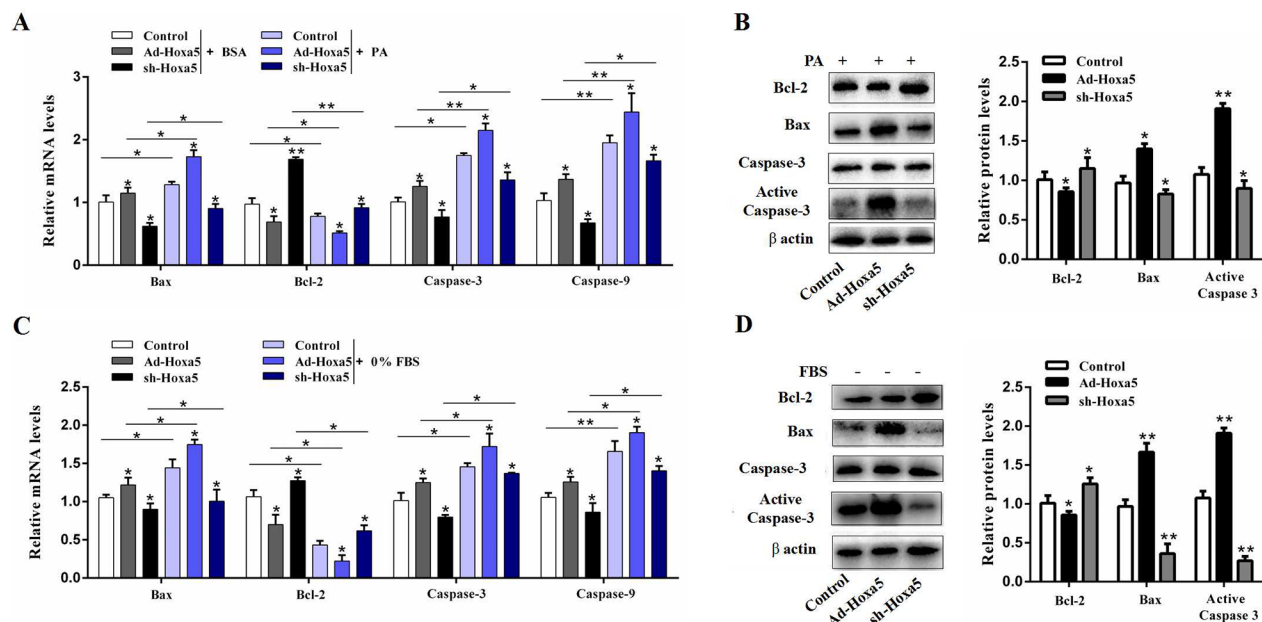


**Figure 4: Hoxa5 aggravated PA- and serum starvation-induced white adipocyte apoptosis.** White adipocytes were pretreated with either Ad-Hoxa5 or sh-Hoxa5. (A, B) Relative mRNA levels of *Bax*, *Bcl-2*, *Caspase-3* and *Caspase-9* (n = 6) (A) and protein levels of Bax, Bcl-2, active Caspase-3 (n = 3) (B) in white adipocytes with 250 nM PA treatment for 24 h. (C, D) Relative mRNA levels of *Bax*, *Bcl-2*, *Caspase-3* and *Caspase-9* (n = 6) (C) and protein levels of Bax, Bcl-2, active Caspase-3 (n = 3) (D) in white adipocytes with serum starvation treatment for 12 h. Values are mean  $\pm$  SEM. \* $P < 0.05$ , \*\* $P < 0.01$  compared with the control.

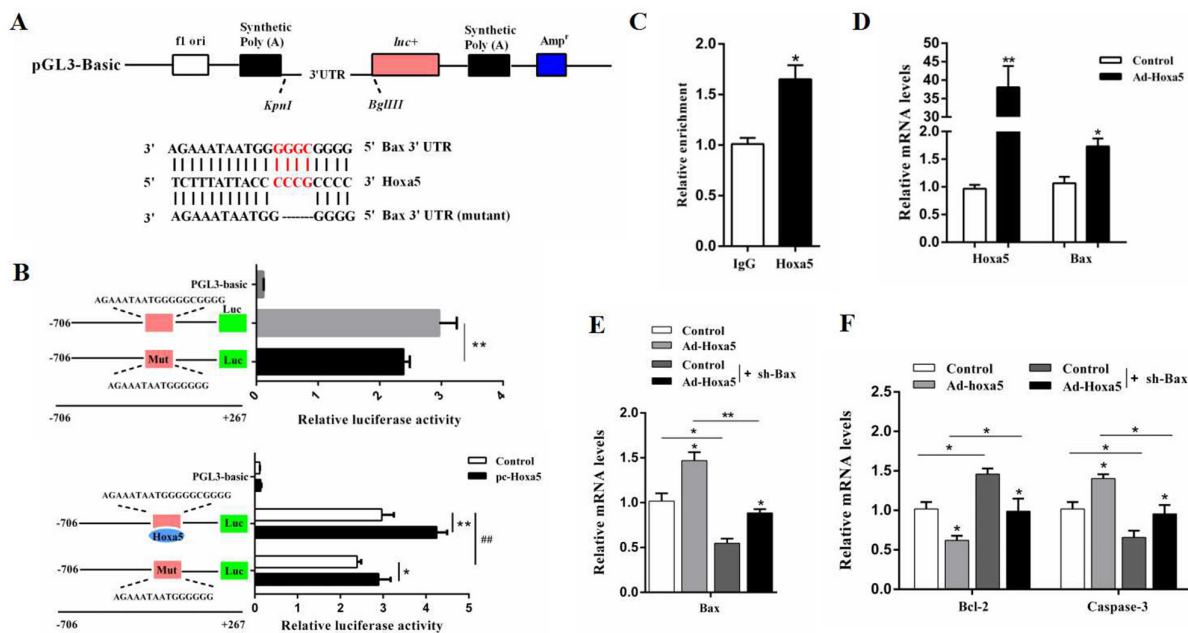


**Figure 5: Hoxa5 promoted apoptosis by elevating *Bax* transcription in white adipocytes.** (A) The construction of the luciferase (Luc) expression vector fused to the 3'UTR and predicted target sites between Hoxa5 and mouse *Bax* 3'UTR. (B) Dual luciferase reporter assay of Hoxa5 and *Bax*. HEK293T cells were transfected with PGL3-basic (control), PGL3-Bax or PGL3-Bax-mutant plasmids (top); HEK293T cells were transfected with PGL3-basic (control), PGL3-Bax or PGL3-Bax-mutant plasmids together with pc-Hoxa5 (bottom) (n = 6). (C) CHIP analysis between Hoxa5 and *Bax* (n = 3). (D) Relative mRNA levels of *Hoxa5* and *Bax* with Ad-Hoxa5 infection of white adipocytes (n = 6). (E, F) Relative mRNA levels of *Bax* (E), *Bcl-2* and *Caspase-3* (F) of white adipocytes after co-transfection with Ad-Hoxa5 and sh-Bax (n = 6). Luciferase activity was corrected for Renilla luciferase activity and normalized to the control activity. PGL3-Bax: fragment of *Bax* promoter region fused to a luciferase reporter, PGL3-Bax-mutant: fragment of mutant *Bax* promoter fused to a luciferase reporter. Values are mean  $\pm$  SEM. \*, # $P < 0.05$ , \*\*, ## $P < 0.01$  compared with the control.

adipocyte apoptosis in mice. Data showed PA injection markedly promoted the mRNA level of *Hoxa5* in iWAT ( $P < 0.01$ ). And, Ad-*Hoxa5* injection also elevated *Hoxa5* mRNA level effectively ( $P < 0.01$ ) (Figure 7A). We then measured the mRNA and protein levels of Bax, Bcl-2 and Caspase-3. And as expected, PA significantly increased apoptosis in iWAT ( $P < 0.05$ ). However, the apoptosis was alleviated after sh-*Hoxa5* injection, and aggravated in Ad-

*Hoxa5* group (Figure 7B-7D). Thus, we concluded *Hoxa5* aggravated PA-induced apoptosis in iWAT of mice.

## DISCUSSION

Excess lipid accumulation, caused by the increased number and volume of adipocytes directly, contributes to obesity, type 2 diabetes, fatty liver and other metabolic

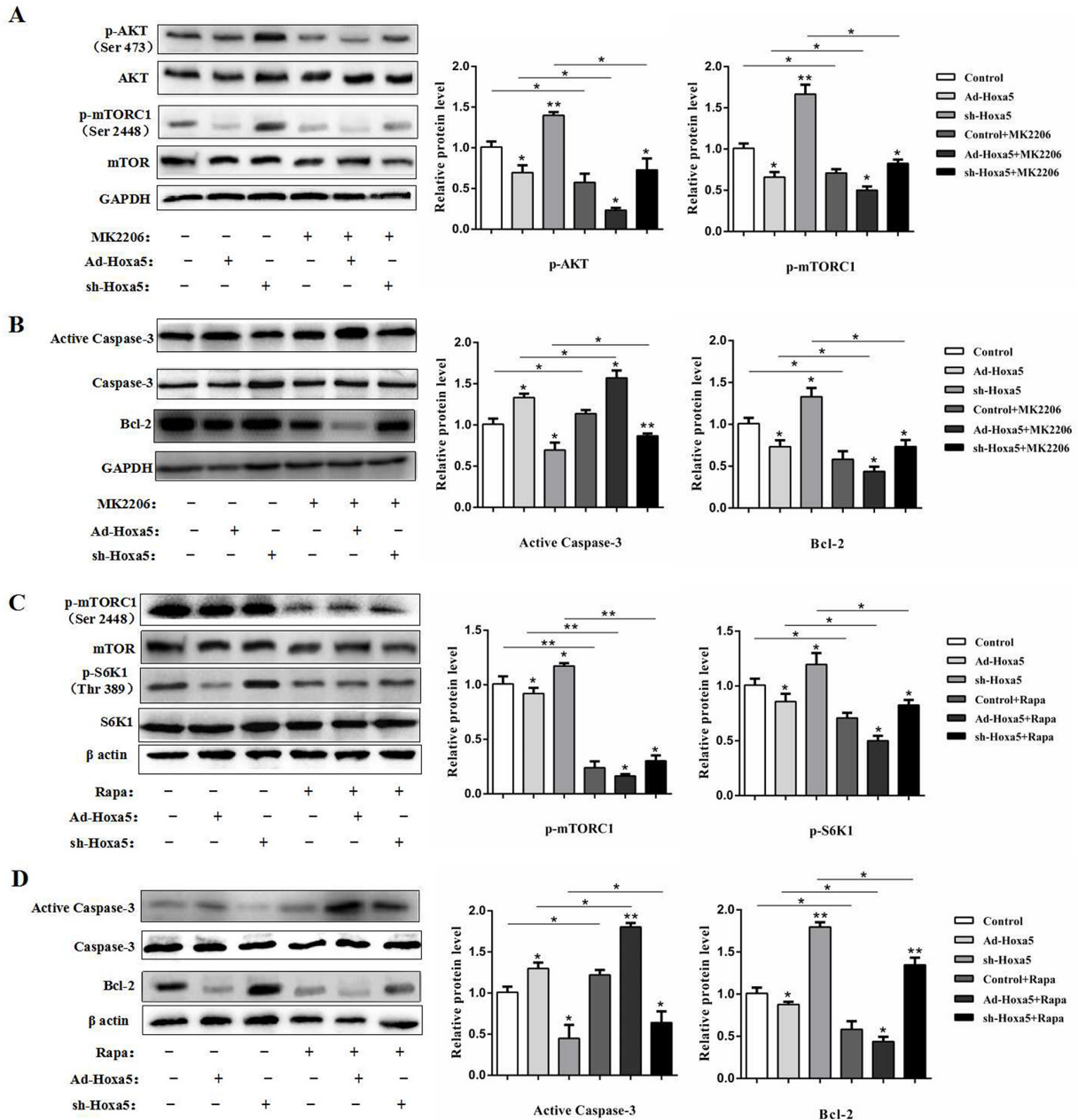


**Figure 6: *Hoxa5* increased white adipocyte apoptosis via the Akt/mTORC1 pathway.** White adipocytes were pretreated with Ad-*Hoxa5* or sh-*Hoxa5*, MK2206 or rapamycin. (A) Relative phosphorylation levels of Akt<sup>Ser473</sup> and mTORC1<sup>Ser2448</sup> with or without MK2206 in each group of white adipocytes (n = 3). (B) Relative protein levels of active Caspase-3 and Bcl-2 with or without MK2206 in each group of white adipocytes (n = 3). (C) Relative phosphorylation levels of mTORC1<sup>Ser2448</sup> and S6K1<sup>Thr389</sup> with or without rapamycin in each group of white adipocytes (n = 3). (D) Relative protein levels of active Caspase-3 and Bcl-2 with or without rapamycin in each group of white adipocytes (n = 3). Values are mean  $\pm$  SEM. \* $P < 0.05$ , \*\* $P < 0.01$  compared with the control.

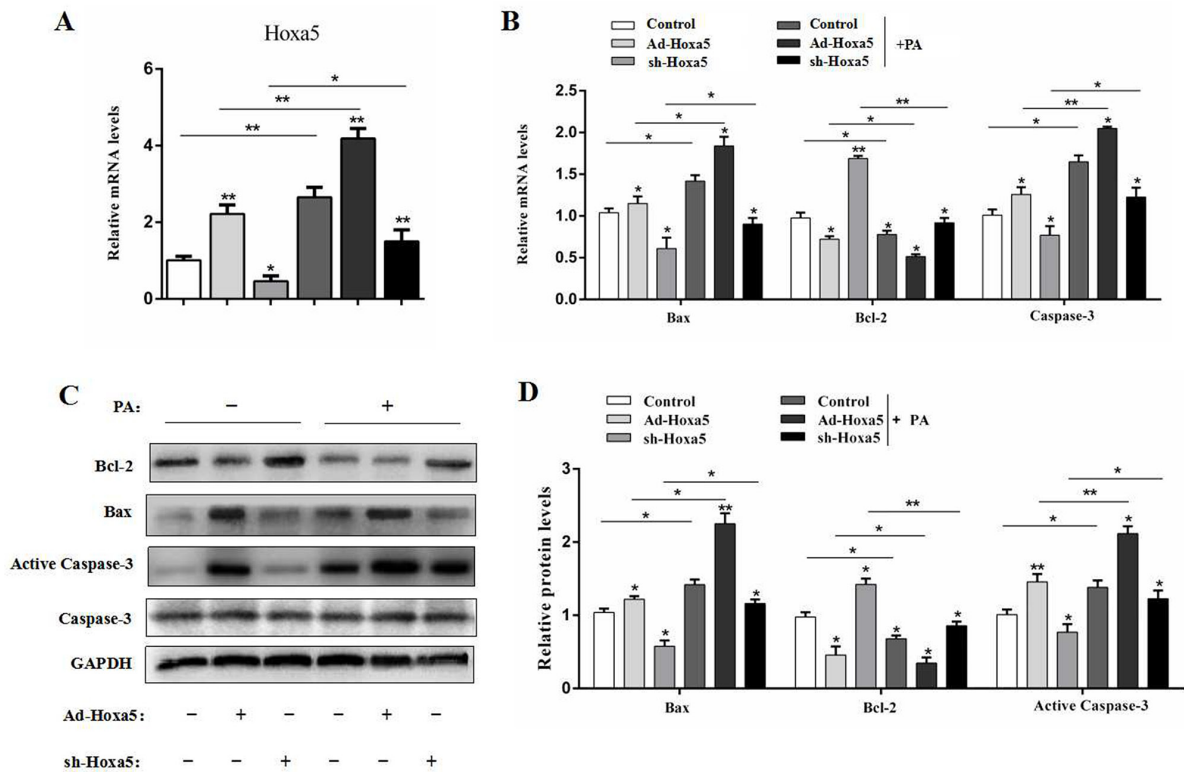


**Figure 7: Hoxa5 promoted PA-induced apoptosis in white adipose tissue of mice.** Seven-week-old mice were intraperitoneally injected either PBS or PA, Ad-Hoxa5 or Sh-Hoxa5. (A, B) Relative mRNA level of *Hoxa5* (A), *Bax*, *Bcl-2* and *Caspase-3* (B) in the iWAT of mice after Ad-Hoxa5 or sh-Hoxa5 and PA or PBS injection once a day for 6 days (n = 6). (C, D) Relative protein levels of Bax, Bcl-2 and Active Caspase-3 in the iWAT of mice after Ad-Hoxa5 or sh-Hoxa5 and PA or PBS injection once a day for 6 days (n = 3). Values are mean  $\pm$  SEM. \* $P < 0.05$ , \*\* $P < 0.01$  compared with the control.

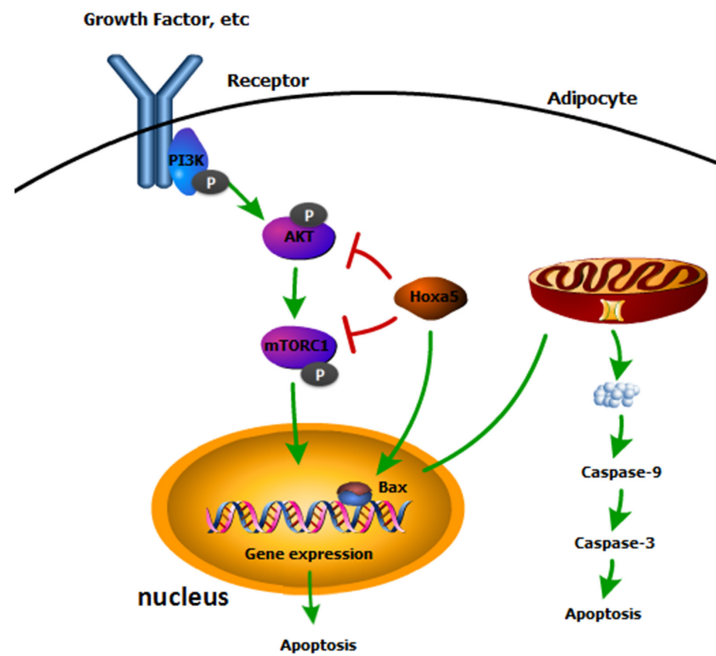


**Figure 8: A summary of the regulation of Hoxa5 on mice white adipocyte apoptosis.** Our data indicated Hoxa5 increased white adipocyte apoptosis by inhibiting Akt/mTORC1 signaling pathway and Hoxa5 promoted transcription of *Bax* to promote mitochondrial apoptosis in white adipocytes of mice.

**Table 1: Primers for real-time quantitative PCR**

<b>Genes</b>	<b>Accession number</b>	<b>Primer sequences (5' to 3')</b>
<i>Bax</i>	NM_007527.3	F: AGACAGGGGCCTTTTGTCTAC R: AATTCGCCGGAGACTCG
<i>Bcl-2</i>	NM_177410.3	F: GCTACCGTCGTGACTTCGC R: CCAGCCTCCGTTATCCTGGA
<i>Bid</i>	NM_007544.3	F: GCCGAGCACATCACAGACC R: TGGCAATGTTGTGGATGATTTCT
<i>Bad</i>	NM_007522.3	F: TGAGCCGAGTGAGCAGGAA R: GCCTCCATGATGACTGTTGGT
<i>Caspase-3</i>	NM_009810.3	F: CTCGCTCTGGTACGGATGTG R: TCCATAAATGACCCCTTCATCA
<i>Caspase-9</i>	NM_015733.5	F: GGCTGTAAACCCCTAGACCA R: TGACGGGTCCAGCTTCACTA
<i>FasL</i>	NM_010177.4	F: CAGCCCATGAATTACCCATGT R: ATTTGTGTTGTGGTCCTTCTTCT
<i>Tnf-α</i>	NM_013693.3	F: CAGGCGGTGCCTATGTCTC R: CGATCACCCCGAAGTTCAGTAG
<i>Caspase-2</i>	NM_007610.2	F: TACTCCCACCGTTGAGCTGT R: CCGTAGCATCTGTGGATAGGC
<i>Caspase-8</i>	NM_001080126.1	F: TGCTTGACTACATCCCACAC R: GTTGCAGTCTAGGAAGTTGACC
<i>Grp78</i>	NM_001163434.1	F: ACTTGGGGACCACCTATTCCT R: GTTGCCCTGATCGTTGGCTA
<i>Chop</i>	NM_007837.4	F: AAGCCTGGTATGAGGATCTGC R: TTCCTGGGGATGAGATATAGGTG
<i>Caspase-7</i>	NM_007611.2	F: AAGACGGAGTTGACGCCAAG R: CCGCAGAGGCATTTCTCTTC
<i>Caspase-12</i>	NM_009808.4	F: TAGGGGAAAGTGCGAGTTTCA R: GGGCCAATCCAGCATTTACCT
<i>Hoxa5</i>	NM_010453.5	F: CTCATTTTTCGGTCGCTATCC R: ATCCATGCCATTGTAGCCGTA
<i>Hoxa4</i>	NM_008265.3	F: CGGTGGTGTACCCCTGGAT R: GCTTAGGTTTCGCTCCGTTAT
<i>Hoxa7</i>	NM_010455.2	F: GCGCTTTTGTAGCAAATACGGC R: GGGATGTTTTGGTCGTAGGAG
<i>Hoxa9</i>	NM_010456.3	F: CCCCRACTTCAGTCCTTGC R: CCAGGAGCGCATATACCTGC
<i>GAPDH</i>	NM_008084.3	F: AGGTCGGTGTGAACGGATTTG R: GGGGTCGTTGATGGCAACA

syndromes [28–30]. In addition to nutritional levels and environmental conditions, the unbalance between cell proliferation and apoptosis of adipocytes might lead to obesity [26].

Apoptosis, or programmed cell death, eliminates unneeded and dangerous cells timely and effectively throughout the lifespan of multicellular organisms [31, 32]. In recent years, many studies focused on the exogenous apoptotic pathway, that is, the DR-mediated pathway and the endogenous apoptotic pathway, that is, the mitochondrial pathway. In addition, they also found other ways involved in regulation of apoptosis, such as ERS-induced and cell cycle arrest-induced apoptosis [33, 34]. Interestingly, in this study, we found Hoxa5 triggered apoptosis through mitochondrial pathway, but not other ways. In the mammal, the Bcl-2 family proteins play a crucial role in regulating caspase activation through mitochondrial pathway. Some external environmental factors stimulate cells to respond to apoptosis signals, resulting in the imbalance of pro- and anti-apoptotic Bcl-2 family members, especially affecting Bax, Bcl-2, Bad and Bid on the mitochondrial membrane [35, 36]. Then mitochondrial proteins including Cytochrome-c (Cyt-c) and second mitochondria-derived activator of caspases (Smac) are released into the cytoplasm. Cyt-c binds to Apaf-1, forming an apoptosome complex with procaspase-9 and Caspase-9 is activated. Subsequently, the activation of downstream caspases results in apoptosis. Parallely, Smac protein binds to the inhibitor of apoptosis protein (IAP), suppressing the inhibitory effect of caspase activity, which promotes the process of apoptosis [34, 37]. Here, we found that Hoxa5 significantly increased the early and late apoptotic cells, decreased the mitochondrial membrane potential and aggravated nuclear genomic DNA fragmentation. Moreover, data showed that Hoxa5 enhanced the expression of pro-apoptotic genes involved in mitochondrial pathway, such as Bax, Bim, Bid, cleaved caspase-9 and cleaved caspase-3. Besides, results also revealed that Hoxa5, as an important transcription factor, bound to *Bax* promoter region and elevated the transcription activity of *Bax*. So, we suggested that Hoxa5 promoted white adipocyte apoptosis through mitochondrial pathway.

Akt and its downstream target mTOR form the core effector of the Akt/mTOR signaling pathway, which is involved in regulating cell proliferation, apoptosis, differentiation and intracellular energy metabolism [38]. It has been found in mammals that mTOR binds to other proteins to form two different complexes, mTORC1 and mTORC2. In contrast, mTORC1 is more sensitive to rapamycin and activates downstream S6 kinase (S6K) and eukaryotic translation initiation factor 4E binding protein 1 (4E-BP1) to regulate cell growth, apoptosis, protein synthesis and cell autophagy [39]. Recent studies have shown that the suppression of mTORC1 phosphorylation by specific inhibitor AZD8055 or rapamycin increases some apoptotic proteins of Bcl-2 family, and then amplifies apoptosis signal through the mitochondrial pathway,

causing the downstream caspases cascade reaction to trigger apoptosis [39–41]. In support of these data, we detected the role of Akt/mTORC1/S6K1 signal pathway and used MK2206 and rapamycin, specific phosphorylation inhibitors of Akt and mTORC1. Results indicated that the promoting effect of Hoxa5 on adipocyte apoptosis was through inhibiting Akt/mTORC1/S6K1 signaling pathway.

In summary, our study revealed that Hoxa5 promoted white adipocyte apoptosis by inhibiting Akt/mTORC1/S6K1 pathway. Also, we found that Hoxa5 elevated the transcription activity of *Bax*, which increased the mitochondrial apoptosis of adipocytes (Figure 8). Our findings might demonstrate a further understanding of regulatory mechanisms of adipocyte apoptosis and provide some novel approaches for therapies of obesity.

## MATERIALS AND METHODS

### Animal study

Six-week-old C57BL/6J male mice were purchased from the Laboratory Animal Center of the Fourth Military Medical University (Xi'an, China). Mice handling protocols were conducted following the guidelines and regulations approved by the Animal Ethics Committee of Northwest A&F University (Yangling, China). Mice were provided with *ad libitum* water and standard chow diet. The animal room was maintained under conditions of temperature at  $25 \pm 1$  °C, humidity at  $55 \pm 5\%$ , and a 12 h light and 12 h dark cycle. Seven-week-old mice were intraperitoneally injected either PBS or palmitate acid (PA, 1  $\mu\text{g/g}$ ) (Sigma, St. Louis, MO, USA) per 2 days for 2 weeks before dark cycle. Body weight and food intake were recorded per 2 days. iWAT and iBAT were removed on the 14<sup>th</sup> day. After intraperitoneal injection of recombinant adenovirus overexpression vector of Hoxa5 (Ad-Hoxa5) and recombinant adenovirus interference vector of Hoxa5 (sh-Hoxa5) to mice for 6 days, iWAT were sampled for future studies.

### Primary adipocyte culture

Inguinal white adipose tissue was harvested, visible fibers and blood vessels were removed, and the adipose tissue was washed three times with a PBS buffer containing 200 U/mL penicillin (Sigma, St. Louis, MO) and 200 U/mL streptomycin (Sigma). White adipocytes were seeded onto 35 mm culture dishes at a density of  $8 \times 10^4$  cells/dish, and cells were maintained in medium containing Dulbecco's modified Eagle's-H21 medium/Ham's F12 (DMEM/F12), 10% FBS (Gibco, Carlsbad, USA) and 1% penicillin-streptomycin and cells were incubated at 37 °C under a humidified atmosphere of 5% CO<sub>2</sub> and 95% air until confluence. The medium was changed every other day. The adipocyte culture was carried out according to our previous publication [42].

## Chemical treatment and vectors infection

For the *in vitro* experiment, white adipocytes were treated with PA (250 nM) or bull serum albumin (BSA, 0.5%, control) for 24 h; serum-free medium or fetal bovine serum (FBS, 10%, control) medium for 12 h to induce apoptosis, and TM (1 µg/mL) for 12 h to create ERS. White adipocytes were infected with Ad-Hoxa5 or sh-Hoxa5 or 24 h or 48 h at the titer of  $1 \times 10^9$  IFU/mL. The recombinant adenovirus vector and interference vector of Hoxa5 (Ad-Hoxa5, sh-Hoxa5), adenovirus interference vector of Bax (sh-Bax) and control vectors were purchased from Gene Pharma (Shanghai, China). For signaling pathway study, the experimental procedure was as described in our previous reports in detail [43]. Briefly, white adipocytes were treated with Akt phosphorylation-specific inhibitor MK2206 (10 µM, Selleck, Houston, USA) and mTORC1 inhibitor rapamycin (10 µM, Selleck, Houston, USA) or DMSO (Promega, Madison, USA) for 6 h, and samples were assessed by Western blot.

## Apoptosis assessment

Cell viability was measured using Cell Counting Kit-8 (CCK-8, Vazyme, Nanjing, China) assay after incubation with PA or adenovirus vectors. After treatment with PA or adenovirus vectors, adipocytes were incubated for 30 min with Hoechst 33342 staining dye (Solarbio, Beijing, China), and washed three times with PBS. Cells were observed by using a Nikon TE2000-U microscope (Nikon, Tokyo, Japan).

The adipocyte apoptosis was measured by FITC-labeled annexin V/PI staining. An annexin V-FITC apoptosis assay kit (Vazyme, Nanjing, China) was used according to the manufacturer's protocol. Afterwards, cells were observed by using a Nikon TE2000-U microscope and the data was analyzed with Image J. The cell percentage of different apoptotic stages was determined by flow cytometry (BD FACScan; BD Biosciences) and data were analyzed using Cell Quest software (BD Biosciences).

The TUNEL assay was performed to detect the fragments of genome DNA by using *in situ* cell death detection kit (Roche, Switzerland). Adipocytes were infected with Ad-Hoxa5 or sh-Hoxa5 for 24 h. Then, adipocytes were trypsinized and suspended in 0.5 mL PBS, and added with 4% (v/v) paraformaldehyde in PBS to fix cells for 30 min at room temperature. Cells were permeabilized with 0.1% TritonX-100 on ice for 2 min and then stained by TUNEL fluorochrome. Cells were observed by using a Nikon TE2000-U microscope and the percentage of positive cells was analyzed with Image J.

## Mitochondrial membrane potential ( $\Delta\Psi_m$ ) measurement

Fluorescent probe JC-1 (Beyotime, Nanjing, China) was used to estimate  $\Delta\Psi_m$ . The experimental procedure

was as described previously [44]. Briefly, cells were incubated at 37 °C for 10 min with 5 µg/mL JC-1, then washed twice with PBS. Images were scanned by a fluorescence microscope (Nikon TE2000-U, Japan). The fluorescence intensity was analyzed with Image J. Also, adipocytes were trypsinized and suspended in 0.5 mL PBS for flow cytometer analysis. JC-1 was excited at 488 nm. JC-1 monomer signal (green) was analyzed at 525 nm and JC-1 aggregates signal (red) was analyzed at 590 nm. The ratio of red/green fluorescent intensity was calculated for the level of  $\Delta\Psi_m$ .

## Promoter reporter assay and dual luciferase reporter assay

The *Bax* promoter sequence was analyzed by using Genomatrix MatInspector. A fragment containing *Bax* - 5' sequence -706 bp ~ +267 bp relative to the transcription initiation site was inserted into a pGL3-basic vector (Takara, Dalian, China), named pGL3-Bax. Mutant *Bax* reporter plasmids were generated using pGL3-Bax plasmid as a template, and a mutagenesis kit (Invitrogen, CA, USA) was used. HEK293T cells were co-transfected with Renilla plasmid, pGL3-basic or pGL3-Bax plasmid (control reporter), and *Hoxa5* overexpression plasmid (pc-Hoxa5). Cells were harvested 48 h after transfection and detected using the Dual-Luciferase Reporter assay system (Promega, Madison, WI, USA) [45].

## ChIP assay

White adipocytes were prepared for chromatin immunoprecipitation (ChIP) assay using a ChIP assay kit (Abcam, Cambridge, UK) according to the manufacturer's protocol. Primary antibodies of Hoxa5 (Abcam) or IgG (Abcam) were used. DNA-protein crosslinking complexes were collected, and purified DNA was subjected to qPCR with SYBR green fluorescent dye (Invitrogen, Carlsbad, CA, USA).

## Real-time quantitative PCR analysis

Total RNA was extracted from adipose tissues (iWAT and iBAT) or white adipocytes using TRIPure Reagent kit (Takara, Dalian, China) according to the manufacturer's instructions. 500 ng of total RNA was reverse transcribed using M-MLV reverse transcriptase kit (Takara, China). Primers were designed by Premier 5.0 and were synthesized by Invitrogen (Table 1, Shanghai, China). Real-time PCR amplification was performed in 25 µL reaction system containing specific primers and SYBR Premix (Vazyme, Nanjing, China) under specific amplification conditions. Amplification reactions were carried out in the ABI StepOne plus™ RT-PCR System (Carlsbad, CA). The levels of mRNA were normalized to Gapdh.  $2^{-\Delta\Delta Ct}$  method was used to analyze the data.

## Western blot analysis

Protein from white adipocytes or white adipose tissue was extracted using lysing buffer. Protein concentration was determined using BCA Protein Assay kit (Beyotime, Nanjing, China). The experimental procedure was as described previously [46]. Briefly, Protein samples (30 µg) were separated by SDS-PAGE and transferred to PVDF nitrocellulose membranes (Millipore, USA), and blocked with 5% Skim Milk Powder/Tween 20/TBST at room temperature for 2 h. Then, primary antibodies against Bcl-2 (bs1511), Cleaved Caspase-9 (bs7070), Cleaved Caspase-3 (bs7004), Gapdh (ap0063), β-actin (ap0060) (Bioworld, CA, USA), Hoxa5 (ab140636), Bax (ab32503), Cytochrome C (ab53056), Akt (ab8805), p-Akt<sup>Ser473</sup> (ab81283), mTOR (ab87540), p-mTORC1<sup>Ser2448</sup> (ab137133), and S6K1 (ab9366), p-S6K1<sup>Thr389</sup> (ab2571) (Abcam, Cambridge, UK) were used to incubate the membranes at 4 °C overnight and the appropriate HRP-conjugated secondary antibodies (Boaoshen, China) were used for 2 h at room temperature. Akt phosphorylation-specific inhibitor MK2206 and mTORC1 inhibitor rapamycin were purchased from Selleck Chemical (USA). Proteins were visualized using chemiluminescent peroxidase substrate (Millipore, USA), and then the blots were quantified using ChemiDoc XRS system (Bio-Rad, USA).

## Statistics

Statistical analyses were performed using SAS v8.0 (SAS Institute, Cary, NC). Data were analyzed using one-way ANOVA procedure. Comparisons among individual means were made by Fisher's least significant difference (LSD). Data are presented as mean ± SEM.  $P < 0.05$  was considered to be significant.

## CONFLICTS OF INTEREST

The authors declare that no conflicts of interest exists.

## GRANT SUPPORT

This work was supported by Major National Scientific Research Projects (2015CB943102) and National Nature Science Foundation of China (31572365).

## REFERENCES

1. Montavon T, Duboule D. Chromatin organization and global regulation of Hox gene clusters. *Philos Trans R Soc Lond B Biol Sci.* 2013; 368:20120367.
2. Chang CJ, Chen YL, Hsieh CH, Liu YJ, Yu SL, Chen JJ, Wang CC. HOXA5 and p53 cooperate to suppress lung cancer cell invasion and serve as good prognostic factors in non-small cell lung cancer. *J Cancer.* 2017; 8:1071-1081.
3. Morgan R, Plowright L, Harrington KJ, Michael A, Pandha HS. Targeting HOX and PBX transcription factors in ovarian cancer. *BMC Cancer.* 2010; 10:89.
4. Gao L, Sun J, Liu F, Zhang H, Ma Y. Higher expression levels of the HOXA9 gene, closely associated with MLL-PTD and EZH2 mutations, predict inferior outcome in acute myeloid leukemia. *OncoTargets Ther.* 2016; 9:711-722.
5. McGinnis W, Krumlauf R. Homeobox genes and axial patterning. *Cell.* 1992; 68:283-302.
6. Mandeville I, Aubin J, LeBlanc M, Lalancette-Hébert M, Janelle MF, Tremblay GM, Jeannotte LM. Impact of the loss of Hoxa5 function on lung alveogenesis. *Am J Pathol.* 2006; 169:1312-1327.
7. Shah N, Sukumar S. The Hox genes and their roles in oncogenesis. *Nat Rev Cancer.* 2010; 10:361-371.
8. Raman V, Martensen SA, Reisman D, Evron E, Odenwald WF, Jaffee E, Marks J, Sukumar S. Compromised HOXA5 function can limit p53 expression in human breast tumors. *Nature.* 2000; 405:974-978.
9. Raman V, Tamori A, Vali M, Zeller K, Korz D, Sukumar S. HOXA5 regulates expression of the progesterone receptor. *J Biol Chem.* 2000; 275:26551-26555.
10. Chen H, Chung S, Sukumar S. HOXA5-induced apoptosis in breast cancer cells is mediated by caspases 2 and 8. *Mol Cell Biol.* 2004; 24:924-935.
11. Wang CC, Su KY, Chen HY, Chang SY, Shen CF, Hsieh CH, Hong QS, Chiang CC, Chang GC, Yu SL, Chen JJ. HOXA5 inhibits metastasis via regulating cytoskeletal remodelling and associates with prolonged survival in non-small-cell lung carcinoma. *PLoS One.* 2015; 10:e0124191.
12. Ordóñez-Morán P, Dafflon C, Imajo M, Nishida E, Huelsken J. HOXA5 counteracts stem cell traits by inhibiting wnt signaling in colorectal cancer. *Cancer Cell.* 2015; 28:815-829.
13. Yang F, Miao L, Mei Y, Wu M. Retinoic acid-induced HOXA5 expression is co-regulated by HuR and miR-130a. *Cell Signal.* 2013; 25:1476-1485.
14. Fu YF, Liu X, Gao M, Zhang YN, Liu J. Endoplasmic reticulum stress induces autophagy and apoptosis while inhibiting proliferation and drug resistance in multiple myeloma through the PI3K/Akt/mTOR signaling pathway. *Oncotarget.* 2017; 8:49380-49394. <https://doi.org/10.18632/oncotarget.17862>.
15. Liu Z, Gan L, Liu G, Chen Y, Wu T, Feng F, Sun C. Sirt1 decreased adipose inflammation by interacting with Akt2 and inhibiting mTOR/S6K1 pathway in mice. *J Lipid Res.* 2016; 57:1373-1381.
16. Gan L, Liu Z, Chen Y, Dan L, Feng F, Liu G, Sun C. α-MSH and Foxc2 promote fatty acid oxidation through C/EBPβ negative transcription in mice adipose tissue. *Sci Rep.* 2016; 6:36661.
17. Bhattacharya I, Ullrich A. Endothelin-1 inhibits adipogenesis: role of phosphorylation of Akt and ERK1/2. *FEBS Lett.* 2006; 580:5765-5771.

18. Kong KA, Yoon H, Kim MH. Akt1 as a putative regulator of Hox genes. *Gene*. 2013; 513:287-291.
19. Lee Y, Lee JY, Kim MH. PI3K/Akt pathway regulates retinoic acid-induced Hox gene expression in F9 cells. *Dev Growth Differ*. 2014; 56:518-525.
20. Wang H, Liu G, Shen D, Ye H, Huang J, Jiao L, Sun Y. HOXA1 enhances the cell proliferation, invasion and metastasis of prostate cancer cells. *Oncol Rep*. 2015; 34:1203-1210.
21. Newland SA, Mohanta S, Clément M, Taleb S, Walker JA, Nus M, Sage AP, Yin C, Hu D, Kitt LL, Finigan AJ, Rodewald HR, Binder CJ, et al. Type-2 innate lymphoid cells control the development of atherosclerosis in mice. *Nat Commun*. 2017; 8:15781.
22. Liu Z, Gan L, Wu T, Feng F, Luo D, Gu H, Liu S, Sun C. Adiponectin reduces ER stress-induced apoptosis through PPAR $\alpha$  transcriptional regulation of ATF2 in mouse adipose. *Cell Death Dis*. 2016; 7:e2487.
23. Goodwin PJ, Stambolic V. Impact of the obesity epidemic on cancer. *Annu Rev Med*. 2015; 66:281-296.
24. Liu C, Fu Y, Li CE, Chen T, Li X. Phycocyanin-functionalized selenium nanoparticles reverse palmitic acid-induced pancreatic  $\beta$  cell apoptosis by enhancing cellular uptake and blocking reactive oxygen species (ROS)-mediated mitochondria dysfunction. *J Agric Food Chem*. 2017; 65:4405-4413.
25. Jiang XS, Chen XM, Wan JM, Gui GB, Ruan XZ, Du XG. Autophagy protects against palmitic acid-induced apoptosis in podocytes *in vitro*. *Sci Rep*. 2017; 7:42764.
26. Gan L, Liu Z, Jin W, Zhou Z, Sun C. Foxc2 enhances proliferation and inhibits apoptosis through activating Akt/mTORC1 signaling pathway in mouse preadipocytes. *J Lipid Res*. 2015; 56:1471-1480.
27. Parrillo L, Costa V, Raciti GA, Longo M, Spinelli R, Esposito R, Nigro C, Vastolo V, Desiderio A, Zatterale F, Ciccodicola A, Formisano P, Miele C, et al. Hoxa5 undergoes dynamic DNA methylation and transcriptional repression in the adipose tissue of mice exposed to high-fat diet. *Int J Obes (Lond)*. 2016; 40:929-937.
28. Furukawa ST, Fujita M, Shimabukuro M, Iwaki Y, Yamada Y, Nakajima O, Nakayama M, Makishima M, Matsuda M, Shimomura I. Increased oxidative stress in obesity and its impact on metabolic syndrome. *J Clin Invest*. 2004; 114:1752-1761.
29. Francés DE, Motiño O, Agrá N, González-Rodríguez Á, Fernández-Álvarez A, Cucarella C, Mayoral R, Castro-Sánchez L, García-Casarrubios E, Boscá L, Carnovale CE, Casado M, Valverde ÁM, Martín-Sanz P. Hepatic cyclooxygenase-2 expression protects against diet-induced steatosis, obesity and insulin resistance. *Diabetes*. 2015; 64:1522-1531.
30. Razavi R, Najafabadi HS, Abdullah S, Smukler S, Arntfield M, van der Kooy D. Diabetes enhances the proliferation of adult pancreatic multipotent progenitor cells and biases their differentiation to more  $\beta$ -cell production. *Diabetes*. 2015; 64:1311-1323.
31. Conradt B, Horvitz HR. The *C. elegans* protein EGL-1 is required for programmed cell death and interacts with the Bcl-2-like protein CED-9. *Cell*. 1998; 93:519-529.
32. Enos RT, Davis JM, Velázquez KT, McClellan JL, Day SD, Carnevale KA, Murphy EA. Influence of dietary saturated fat content on adiposity, macrophage behavior, inflammation, and metabolism: composition matters. *J Lipid Res*. 2013; 54:152-163.
33. Hyman BT, Yuan J. Apoptotic and non-apoptotic roles of caspases in neuronal physiology and pathophysiology. *Nat Rev Neurosci*. 2012; 13:395-406.
34. Arya R, White K. Cell death in development: signaling pathways and core mechanisms. *Semin Cell Dev Biol*. 2015; 39:12-19.
35. White K, Grether ME, Abrams JM, Young L, Farrell K, Steller H. Genetic control of programmed cell death in *Drosophila*. *Science*. 1994; 264:677-683.
36. Yuan J, Kroemer G. Alternative cell death mechanisms in development and beyond. *Genes Dev*. 2010; 24:2592-2602.
37. Tarasenko TN, Pacheco SE, Koenig MK, Gomez-Rodriguez J, Kapnick SM, Diaz F, Zervas PM, Barca E, Sudderth J, DeBerardinis RJ, Covian R, Balaban RS, DiMauro S, McGuire PJ. Cytochrome c oxidase activity is a metabolic checkpoint that regulates cell fate decisions during T cell activation and differentiation. *Cell Metab*. 2017; 25:1254-1268.
38. Bhattacharya I, Ullrich A. Endothelin-1 inhibits adipogenesis: role of phosphorylation of Akt and ERK1/2. *FEBS Lett*. 2006; 580:5765-5771.
39. Laplante M, Sabatini DM. mTOR signaling in growth control and disease. *Cell*. 2012; 149:274-293.
40. Qian J, Chen Y, Meng T, Ma L, Meng L, Wang X, Yu T, Zask A, Shen J, Yu K. Molecular regulation of apoptotic machinery and lipid metabolism by mTORC1/mTORC2 dual inhibitors in preclinical models of HER2+/PIK3CAmut breast cancer. *Oncotarget*. 2016; 7:67071-67086. <https://doi.org/10.18632/oncotarget.11490>.
41. Reusch JE, Klemm DJ. Inhibition of cAMP-response element-binding protein activity decreases protein kinase B/Akt expression in 3T3-L1 adipocytes and induces apoptosis. *J Biol Chem*. 2002; 277:1426-1432.
42. Gan L, Liu Z, Cao W, Zhang Z, Sun C. FABP4 reversed the regulation of leptin on mitochondrial fatty acid oxidation in mice adipocytes. *Sci Rep*. 2015; 5:13588.
43. Liu Z, Gan L, Xu Y, Luo D, Ren Q, Wu S, Sun C. Melatonin alleviates inflammasome-induced pyroptosis through inhibiting NF- $\kappa$ B/GSDMD signal in mice adipose tissue. *J Pineal Res*. 2017; 63. <https://doi.org/10.1111/jpi.12414>.
44. Cao W, Li M, Wu T, Feng F, Feng T, Xu Y, Sun C.  $\alpha$ MSH prevents ROS-induced apoptosis by inhibiting Foxo1/mTORC2 in mice adipose tissue. *Oncotarget*. 2017; 8:40872-40884. <https://doi.org/10.18632/oncotarget.16606>.

45. Liu G, Li M, Saeed M, Xu Y, Ren Q, Sun C.  $\alpha$ MSH inhibits adipose inflammation via reducing FoxOs transcription and blocking Akt/JNK pathway in mice. *Oncotarget*. 2017; 8:47642-47654. <https://doi.org/10.18632/oncotarget.17465>.

46. Gan L, Liu Z, Wu T, Feng F, Sun C.  $\alpha$ MSH promotes preadipocyte proliferation by alleviating ER stress-induced leptin resistance and by activating Notch1 signal in mice. *Biochim Biophys Acta*. 2017; 1863:231-238.